MM3 MODELING OF ALDOPENTOSE PYRANOSE RINGS

Michael K. Dowd,[a,*] William M. Rockey,[b] Alfred D. French,[a] and Peter J. Reilly[b]

[a]Southern Regional Research Center, ARS, USDA, 1100 Robert E. Lee Blvd., New Orleans, LA 70179, USA

[b]Department of Chemical Engineering, Iowa State University, Ames, IA 50011, USA

ABSTRACT

MM3 (version 1992, $\varepsilon = 3.0$) was used to study the ring conformations of D-xylopyranose, D-lyxopyranose and D-arabinopyranose. The energy surfaces exhibit low-energy regions corresponding to chair and skew forms with high-energy barriers between these regions corresponding to envelope and half-chair forms. The lowest energy conformer is $^4C_1$ for α- and β-xylopyranose and α- and β-lyxopyranose, and the lowest energy conformer is $^1C_4$ for α- and β-arabinopyranose. Only α-lyxopyranose exhibits a secondary low-energy region ($^1C_4$) within 1 kcal/mol of its global minimum. Overall, the results are in good agreement with NMR and crystallographic results. For many of these molecules, skew conformations are found with relatively low energies (2.5 to 4 kcal/mol above lowest energy chair form). The ^2S_O and $^1C_4$ conformers of crystalline benzoyl derivatives of xylopyranose are in secondary low-energy regions on the β-xylopyranose surface, within 3.8 kcal/mol of the global $^4C_1$ minimum.

INTRODUCTION

Previously, we modeled the pyranosyl ring shapes of the D-aldohexoses with the molecular mechanics program MM3.[1] In general, MM3 predicted the shapes of these cyclic structures well. All of the β-anomers favored the $^4C_1$ conformation, as did most of the α-anomers. For the hexoses existing in multiple forms, e.g. α-idopyranose and α-altropyranose, the model predicted multiple forms. However, the conformer distribution predicted for these molecules was not always in exact agreement with the distributions predicted from NMR results, signifying the effects of modeling error, including neglected solvation and entropic effects. In addition, a comparison of the predicted energies for the anomers indicated that the equatorially configured β-structures were systematically overpredicted.

A better test of a potential energy function for predicting carbohydrate ring forms would be a series of pyranosyl structures known to be more variable in conformational preference. The aldopyranosyl pentoses, which lack the bulky hydroxymethyl group, represent such a series. By NMR,[2,3] α- and β-xylopyranose and β-lyxopyranose exist predominately in the $^4C_1$ form; α- and β-arabinopyranose exist predominately in the $^1C_4$ form; and α-lyxopyranose exists as a mixture of the two chair forms. Ribopyranose, which has already been studied with MM3,[4] is also found as a mixture of chair forms. This series appears to be a good test of the ability of potential functions to reproduce ring conformations.

In addition to the goal of validating molecular models, there is interest in understanding how saccharides interact with proteins and how these interactions facilitate enzyme kinetics. In part,

this stems from the need to improve enzyme stability or to alter reaction conditions. Xylanase is of commercial interest because it reduces the need for chlorine bleaching in paper pulping.[5,6] A number of xylanase structures with xylan fragments or related derivatives bound to the active site have now been solved by diffraction crystallography, and these structures suggest that bound xlyose rings can have non-chair conformations during hydrolysis.[7-9] An understanding of the conformational preferences of xylopyranose may be important for understanding the activity and specificity of these enzymes.

METHODS

The computational methods used in this work have been described in previous publications and will only be outlined here.[1,4] To be consistent with those calculations, the 1992 version of MM3[10-12] was used with an elevated dielectric constant ($\varepsilon = 3.0$). The elevated dielectric constant was used to reduce the strength of intramolecular hydrogen bonding and better mimic carbohydrates in condensed-phase systems.[13] Planar ring structures were initially generated with PC-Model (Serena Software, Bloomington, IN). These structures were then used to create puckered rings by moving three alternating ring atoms and their connected substituents perpendicular to the initial ring plane. This was accomplished by orienting the planar ring into the *xy*-plane and adjusting the *z*-coordinates of the atoms to be shifted. The atoms were moved over a range of -0.8 Å to +0.8 Å in 0.1 Å increments, which was sufficient to cover all likely ring shapes. For each ring, all three staggered gauche conformations of the four secondary hydroxyl groups were also varied. Combined with the different combinations of ring shape, this yielded a total of 397,872 ($17^3 \times 3^4$) starting structures for each monosaccharide. Ring pucker was

maintained during the energy minimization by fixing the z-coordinates of the six ring atoms. All other degrees of freedom were allowed to relax. These optimizations were conducted with the block-diagonal Newton-Raphson method (MM3 Option 1) and the default optimization criteria. The system of Cremer and Pople (q, ϕ, θ) was used to quantify ring shape.[14]

From the full set of optimized structures, a Pickett-Strauss *plate carrée* representation (ϕ, θ) of the Cremer and Pople puckering sphere was generated.[15] To construct this two-dimensional representation, the data was sorted into 10° x 10° regions of ϕ and θ, regardless of the value of q or orientation of the individual exocyclic groups. The lowest energy conformer from each region was selected, and the resulting grid of points was plotted using SURFER (Golden Software, Golden, CO). Positions of the characteristic conformers (chairs, boats, skews, etc.) within this two-dimensional space are shown in Fig. 1.

The Pickett-Strauss surface distorts some aspects of the puckering sphere. Most affected are the two poles (i.e. the chair conformers), which are transformed into the top and bottom y-axes. In effect, the points representing the poles are stretched into lines corresponding to the two horizontal boundaries. Because the system used to generate the puckered rings evenly samples the puckering sphere, the transformation results in a low density of data points near the two chair regions. This results in some distortion of the contour lines near these boundaries.

To find local minima, the local low-energy regions were identified from the Pickett-Strauss surfaces. Molecules with these ring shapes were built with all 81 (3^4) sets of staggered exocyclic orientations. All of these structures were freely optimized to determine the lowest-energy form.

If any of the structures from one local region optimized to a different area of the puckering space, the region was not considered to have a local minimum. The Karplus equations of Haasnoot et al.[16] were used to calculate proton-proton coupling constants for these structures.

The Cambridge Crystal Structure Database[17] was searched to identify related crystal structures. If there were multiple entries within the database, only the most recent determination was included in the analysis, and neutron diffraction determinations were used in preference to x-ray determinations. Structures for compounds containing L-sugars were included after converting the puckering parameters ($\phi_D = 180° - \phi_L$, $\theta_D = 180° - \theta_L$) to account for the change in absolute configuration. The Protein Data Bank[18] was searched for structures with bound xylose rings.

RESULTS AND DISCUSSION

All three pyranosyl energy surfaces (Figs. 2-4) have low-energy regions corresponding to chair and skew forms. The half-chair and envelope forms are relatively high energy and form barriers between the low-energy regions. The MM3 minima for these monosaccharides are reported in Table 1, and selected low-energy structures are shown in Fig. 5.

For both α- and β-xylopyranose, the lowest-energy ring conformer is $^4C_1$. The second-lowest energy conformer for α-xylopyranose is $^1C_4$ and for β-xylopyranose is ^2S_O. These forms are 1.7 and 2.6 kcal higher in energy, respectively. The $^1C_4$ form of β-xylopyranose is the third lowest energy form at 3.8 kcal/mol. The energy differences between the two chair forms are much smaller for xylopyranose than for glucopyranose,[1] demonstrating the large energy penalty for

having the bulky hydroxymethyl side group in an axial orientation. Nevertheless, because the $^4C_1$ conformation dominates the distribution, the calculated coupling constants for the $^4C_1$ form and the conformational average are similar. Both sets of coupling constants are in good agreement with NMR results (Table 1), with a root-mean-square (rms) deviation between the calculated and experimental coupling constants of 0.6 Hz for α-xylopyranose and 0.4 Hz for β-xylopyranose.

Numerous single crystal structures exist for molecules that contain xylopyranosyl rings.[19-42] Most of these structures have $^4C_1$ forms (Fig. 2). Benzoyl derivatives, however, are exceptions.[28,29] For these molecules ^2S_O and $^1C_4$ ring shapes are found, apparently because of stabilization induced by intramolecular stacking of the benzoyl rings in these conformations. Both ring shapes correspond to secondary minima on the β-xylopyranosyl MM3 energy surface (Fig. 2b). The experimental observation of these alternative conformers for xylose derivatives supports the relatively low energies calculated by MM3 for these regions.

In addition to single crystal structures, a number of enzymes have been crystallized with bound xylosyl moieties.[7-9] Although bound subunits are generally less accurately determined in protein diffraction studies than in small-molecule diffraction studies, non-chair xylose ring shapes have been reported in these structures by different research groups.[8,9] In these studies, the xylose ring in the -1 subsite of the family 11 xylanases was observed in a $^{2,5}B$ conformation. This conformation appears to facilitate the formation of an oxo-carbenium ion transition intermediate, which is key to the proposed double displacement catalytic mechanism that accounts for the retention of the β-xylose configuration during hydrolysis. The observed $^{2,5}B$ boat can be obtained from the relatively low-energy ^2S_O form by the downward movement of the anomeric carbon as

it forms the covalent xylose-glutamic acid bridge of the intermediate. Small downward shifts of the O-5 and C-2 ring atoms and the C-2 and C-3 hydroxyl groups are required for this conformational change, but no movement of the C-4 oxygen and its covalently bound oligosaccharide moiety is needed. In terms of puckering parameters, the ϕ angle is reduced from ~150° in the $^{2}S_{O}$ form to ~120° in the $^{2,5}B$ form (Fig. 1), and the MM3 energy change for this conversion is only 2-3 kcal/mol (Fig. 2). Sidhu et al.[9] have proposed an enzyme-mediated ring conversion pathway of $^{4}C_{1} \rightarrow {}^{2}H_{3} \rightarrow {}^{2}S_{O} \rightarrow {}^{2,5}B$ for the formation of this intermediate. However, the relatively low energy of the $^{2}S_{O}$ form (2.6 kcal/mol) may indicate that this conformer exists in solution in a concentration sufficient to allow for the direct binding of this form to the enzyme. In this instance, the enzyme would not need to induce the conformational change through the $^{2}H_{3}$ form, which has a much higher relative energy.

Both anomers of arabinopyranose have $^{1}C_{4}$ lowest energy conformations and $^{4}C_{1}$ second lowest-energy conformations (Fig. 3). For the β-anomer, the $^{4}C_{1}$ form, which has the C-1 hydroxyl group in an equatorial position, is only 1.45 kcal/mol above the global minimum region. Consequently, a small amount (<10%) of this form may exist in solution. The NMR coupling constants calculated for the $^{1}C_{4}$ chair and the conformational equilibrium are in good agreement with experimental values (Table 1). The rms deviation between the experimental and calculated coupling constants for the α- and β-anomers are 0.6 and 0.4 Hz, respectively. In addition, all reported arabinopyranosyl crystal structures[43-52] have $^{1}C_{4}$ conformations (Fig. 3).

The α-D-lyxopyranose surface has a $^{4}C_{1}$ global low-energy region and a $^{1}C_{4}$ secondary low-energy region (Fig. 4a). The energy difference between these two forms is 0.9 kcal/mol (Table

1), indicating that both of the chairs are likely to exist in equilibrium. Except for J_{23}, which has a value of ~3 Hz for either chair, the reported coupling constants are between the values for the two chair forms, which also indicates that both chairs co-exist in solution. Based on the MM3 energies of the local minima, the model predicts an 83%/17% distribution of the $^4C_1$ and $^1C_4$ forms, which appears to underpredict the $^1C_4$ form. As a result, the rms deviation between the calculated and experimental coupling constants is relatively large (1.3 Hz). A least squares best-fit model of the two chairs to the experimental coupling constants improves the fit (0.7 Hz deviation) and yields a 62%/38% ratio of the $^4C_1$ and $^1C_4$ forms. Crystalline acetyl and methyl derivatives of α-D-lyxopyranose[53,54] are both found in $^4C_1$ conformations. MM3 calculations for β-lyxopyranose suggest that the $^4C_1$ form is most likely ring shape. The calculated NMR coupling constants are in reasonable agreement with experimental results (0.7 Hz rms deviation), and the crystal structures for β-L-lyxopyranose[55] and methyl-2,3,4-triacetyl-β-D-lyxopyranoside[56] are also found in the $^4C_1$ form. The second low-energy region for β-D-lyxopyranose is the $^1C_4$, which is 2.6 kcal/mol above the global minimum.

Anomeric ratios can be estimated from the average energies of the conformer populations for each monosaccharide. For xylopyranose, the distribution is calculated to be 14% α-anomer and 86% β-anomer. Compared with the experimental ratio in D_2O (37% α-anomer/63% β-anomer),[3] the β-anomeric form is overpredicted. For lyxopyranose, the calculated distribution is 48% α-anomer and 52% β-anomer, and again the β-form is overpredicted compared to the distribution in D_2O (71% α-anomer/29% β-anomer).[3] A similar difference was previously found to occur for the aldohexoses.[1] For arabinopyranose, the calculated distribution is 82% α-anomer and 18% β-

anomer. In this case, however, the β-anomer is underpredicted in comparison to NMR results in D_2O (63% α-anomer/37% β-anomer).[3]

The systematic difference in the predicted anomeric ratios appears to indicate a small error in the MM3 potential function. For most of the hexoses, and for xylose and lyxose, MM3 energies overpredict the β-pyranosyl form. For these molecules, both anomers are found predominately in the $^4C_1$ form by calculation. For arabinose, MM3 underpredicts the β-pyranosyl form, and in this case both anomers exist predominately in the $^1C_4$ form by calculation. For idopyranose and altropyranose, the MM3 calculated anomer distributions appear to be very close to experimental values. These molecules model as a conformational equilibrium that includes significant amounts of both chair forms, which appears to dampen the effect. All of the overpredicted forms, β-anomers for structures in $^4C_1$ and α-anomers for structures in $^1C_4$, have equatorial orientations of the glycosidic C-1–O bond and *trans* orientations of this bond relative to the C-5–O-5 bond. The underpredicted forms, in contrast, all have axial orientations of the glycosidic hydroxyl group and *gauche* orientations relative to the C-5–O-5 bond. Because the torsional functions associated with the anomeric sequences (O–C–O–H and O–C–O–C) have been especially difficult to model, this functionality is likely responsible for the calculated differences. The analysis, however, is complicated because MM3 also overpredicts the axial form of 2-hydroxytetrahydropyran relative to experiment.[1] Recent ab initio results highlight these effects, and some improvement in the modeling of the anomeric region for disaccharides has been achieved by a hybrid QM/MM approach that in principle corrects for errors in the molecular mechanics modeling of anomeric sequences.[57] In any case, the magnitude of the energy

discrepancy in the MM3 calculation is small and is on the order of magnitude (<1 kcal/mol) of the uncertainty of the quantum mechanical calculations.

There has been considerable debate regarding the importance of solvent and entropic effects on the conformation of small carbohydrates. Inclusion of these "additional" influences is often used to compensate for discrepancies between experimental data and the underlying computational method. With MM3, monosaccharide rings are modeled reasonably well without needing to incorporate other effects. The only accommodation to environmental forces is an increase in the bulk dielectric constant. The principle effect of this is to reduce the strength of intramolecular hydrogen bonds, which may reduce entropy differences that arise because of preferred intramolecular hydrogen bond orientations. In addition, although some effort was made to limit the influence of intermolecular effects in parameterizing MM3, the parameters are derived from a wide variety of experimental and computational data and some external influences may have crept into the model. Consequently, it cannot be absolutely concluded that intermolecular effects and entropy differences are small for the various conformers of these structures.

CONCLUSIONS

MM3 (version 1992, $\varepsilon = 3.0$) was used to study the ring puckering of the two anomeric forms of D-xylopyranose, D-lyxopyranose, and D-arabinopyranose. The modeling indicates that α- and β-xylopyranose and β-lyxopyranose exist predominately in the $^4C_1$ form, that α- and β-arabinopyranose exists predominately in the $^1C_4$ form, and that α-lyxopyranose exists as an equilibrium between the two chair forms. The predicted conformers are in good agreement with those

expected from NMR coupling constants and crystallographic data. For the pentoses, secondary conformations are lower in energy than they were for the hexoses, demonstrating the influence of the C-6 hydroxymethyl group on hexose conformation. A systematic error in the estimation of anomer ratios appears to be related to difficulties in parameterizing some torsion sequences.

REFERENCES

1. Dowd, M.K.; French, A.D.; Reilly, P.J. Modeling of aldopyranosyl ring puckering with MM3(92). Carbohydr. Res. **1994**, *264*, 1-19.
2. Bock, K.; Thøgersen, H. Nuclear magnetic resonance spectroscopy in the study of mono- and oligosaccharides. Ann. Rep. NMR Spectros. **1982**, *13*, 1-57.
3. Angyal, S.J. The composition of reducing sugars in solution. Adv. Carbohydr. Chem. Biochem. **1984**, *42*, 15-68.
4. Dowd, M.K.; French, A.D.; Reilly, P.J. MM3 modeling of ribose and 2-deoxyribose ring puckering. J. Carbohydr. Chem., **2000**, *19*(9), 1091-1114.
5. Farrell, R.L.; Skerker, P.S. Chlorine-free bleaching with Cartazyme™ HS treatment. In *Xylans and xylanases*. Visser, J., Ed.; Elsevier Science Publications: Amsterdam, **1992**, 315-324.
6. Paice, M.G.; Gurnagul, N.; Page, D.H.; Jurasek, L. Mechanism of hemicellulose-directed prebleaching of kraft pulps. Enzyme Microb. Technol. **1992**, *14*, 272-276.
7. Wakarchuk, W.W.; Campbell, R.L.; Sung, W.L.; Davoodi, J.; Yaguchi, M. Mutational and crystallographic analyses of the active site residues of the *Bacillus circulans* xylanase. Prot. Sci. **1994**, *3*, 467-475.

4. Dowd, M.K.; French, A.D.; Reilly, P.J. MM3 modeling of ribose and 2-deoxyribose ring puckering. J. Carbohydr. Chem., **2000**, *19*(9), 1091-1114.

5. Farrell, R.L.; Skerker, P.S. Chlorine-free bleaching with Cartazyme^{TM} HS treatment. In *Xylans and xylanases*. Visser, J., Ed.; Elsevier Science Publications: Amsterdam, **1992**, 315-324.

6. Paice, M.G.; Gurnagul, N.; Page, D.H.; Jurasek, L. Mechanism of hemicellulose-directed prebleaching of kraft pulps. Enzyme Microb. Technol. **1992**, *14*, 272-276.

7. Wakarchuk, W.W.; Campbell, R.L.; Sung, W.L.; Davoodi, J.; Yaguchi, M. Mutational and crystallographic analyses of the active site residues of the *Bacillus circulans* xylanase. Prot. Sci. **1994**, *3*, 467-475.

8. Sabini, E.; Sulzenbacher, G.; Dauter, M.; Dauter, M.; Jørgensen, P.L.; Schülein, M.; Dupont, C.; Davies, G.; Wilson, K.S. Catalysis and specificity in enzymatic glycoside hydrolysis: a $^{2,5}B$ conformation for the glycosyl-enzyme intermediate revealed by the structure of the *Bacillus agaradhaerens* family 11 xylanase. Chem. Biol. **1999**, *6*(7), 483-492.

9. Sidhu, G.; Withers, S.G.; Nguyen, N.T.; McIntosh, L.P.; Ziser, L.; Brayer, G.D. Sugar ring distortion in the glycosyl-enzyme intermediate of a family G/11 xylanase. Biochemistry **1999**, *38*(17), 5346-5354.

10. Allinger, N.L.; Yuh, Y.H.; Lii, J.H. Molecular mechanics. The MM3 force field for hydrocarbons. 1. J. Am. Chem. Soc. **1989**, *111*(23), 8551-8566.

11. Lii, J.H.; Allinger, N.L. The MM3 force field for hydrocarbons. 2. Vibrational frequencies and thermodynamics. J. Am. Chem. Soc. **1989**, *111*(23), 8566-8575.

12. Allinger, N.L.; Rahman, M.; Lii, J.H. A molecular mechanics force field (MM3) for alcohols and ethers. J. Am. Chem. Soc. **1990**, *112*(23), 8293-8307.

13. Cremer, D.; Pople, J.A. A general definition of ring puckering coordinates. J. Am. Chem. Soc. **1975**, *97*(6), 1354-1358.

14. Haasnoot, C.A.G.; de Leeuw, F.A.A.M.; Altona, C. The relationship between proton-proton NMR coupling constants and substituent electronegativities–I. Tetrahedron **1980**, *36*(19H), 2783-2792.

15. Pickett, H.M.; Strauss, H.L. Conformational structure, energy, and inversion rates of cyclohexane and some related oxanes. J. Am. Chem. Soc. **1970**, *92*, 7281-7290.

16. Allen, F.H.; Kennard, O. 3D search and research using the Cambridge Structural Data-base. Chem. Design Automation News **1993**, *8*, 1,31-37.

17. Berman, H.M.; Westbrook, J.; Feng, Z.; Gilliland, G.; Bhat, T.N.; Wessig, H.; Shindyalov, I.N.; Bourne, P.E. The protein data bank. Nucleic Acids Res. **2000**, *28*, 235-242.

18. Richards, G.F. An X-ray crystallographic study of a metal-carbohydrate complex: α-D-xylose•$CaCl_2$•$3H_2O$. Carbohydr. Res. **1973**, *26*, 448-449.

19. Moran R.A.; Richards, G.F. The crystal and molecular structure of an aldotriourionic acid trihydrate: *O*-(4-*O*-Methyl-α-D-glucopyranosyluronic acid)-(1-2)-*O*-β-D-xylopyranosyl-(1-4)-D-xylopyranose trihydrate. Acta Crystallogr., Sect. B **1973**, *29*, 2770-2783.

20. Leung, F.; Marchessault, R.H. Crystal structure of β-D,1 → 4 xylobiose hexahydrate. Can. J. Chem. **1973**, *51*, 1215-1222.

21. James, V.J.; Stevens, J.D. Methyl 2,3,4-tri-*O*-acetyl-α-D-xylopyranoside. $C_{12}H_{18}O_8$. Cryst. Struct. Commun. **1974**, *3*, 27-30.

22. Delbaere, L.T.J.; Kamenar, B.; Prout, K. The crystal and molecular structure of *O*-(β-D-xylopyranosyl)-L-serine and its copper(II) complex. Acta Crystallogr., Sect. B **1975**, *31*, 862-865.

23. James, V.J.; Nimgirawath, K.; Stevens, J.D. 1,2,3,4-Tetra-*O*-acetyl-β-D-xylopyranose. $C_{13}H_{18}O_9$. Cryst. Struct. Commun. **1976**, *5*, 851-856.

24. Takagi, S.; Jeffrey, G.A. A neutron diffraction refinement of the crystal structures of β-L-arabinose and methyl β-D-xylopyranoside. Acta Crystallogr., Sect. B **1977**, *33*, 3033-3040.

25. Takagi, S.; Jeffrey, G.A. Methyl β-D-xylopyranoside. Acta Crystallogr., Sect. B **1978**, *34*, 3104-3107.

26. Takagi, S.; Jeffrey, G.A. α-L-Xylopyranoside: A neutron diffraction refinement. Acta Crystallogr., Sect. B **1979**, *35*, 1482-1486.

27. Luger, P.; Kothe, G.; Vangehr, K.; Paulsen, H.; Heiker, F.R. Konformationen von 1,2,3,4-tetra-*O*-benzoyl-β-D-xylopyranose, 1,5-anhydro-2,3,4-tri-*O*-benzoylxylitol und 1,5-anhydro-2,3,4-tri-*O*-benzoylribitol. Carbohydr. Res. **1979**, *68*, 207-223.

28. Vangehr, K.; Luger, P.; Paulsen, H. Twist-boat-konformation von methyl-2,3,4-tri-*O*-benzoyl-β-D-xylopyranosid im kristall. Chem. Ber. **1980**, *113*, 2609-2615.

29. Vorontsova, L.G.; Dekaprilevich, M.O.; Chizhov, O.S. An x-ray diffraction structural study of 2,3,4-tri-*O*-acetyl-β-methyl-D-xylopyranoside. Izv. Akad. Nauk SRRC, Ser. Khim. **1985**, (4), 824-826.

30. Vorontsova, L.G.; Dekaprilevich, M.O.; Chizhov, O.S. Molecular and crystal structure of β-methyl-2,3-di-*O*-acetyl-4-*O*-trityl-D-xylopyranoside. Izv. Akad. Nauk SRRC, Ser. Khim. **1985**, (7), 1563-1567.

31. Tavanaiepour, I.; Watson, W.H.; Gao, F.; Mabry, T.J. Structure of a diterpene *ent*-Labdane xyloside. Acta Crystallogr., Sect. C **1987**, *43*, 754-756.

32. Beagley, B.; Larson, D.S.; Pritchard, R.G.; Stoodley, R.J. Asymmetric Diels-Alder reactions. Part 5. Influence of sugar substituents upon the diastereofacial reactivity of (*E*)-3-(*t*-butyldimethylsiloxy)-1-(D-glucopyranosyloxy)buta-1,3-dienes. J. Chem. Soc., Perkin Trans. 1 **1990**, 3113-3127.

33. Il'in, S.G.; Reshetnyak, M.V.; Shedrin, A.P.; Struchkov, Y.T.; Kapustina, I.I.; Stonik, V.A.; Elyakov, G.B. The crystal and molecular structure of 6α,8β,15β-tridydroxy-3β-24R-di(*O*-β-D-xylopyranosyl)-5α-cholest-22(23)-ene trihydrate. Dokl. Akad. Nauk **1990**, *312*(3), 637-639.

34. van der Sluis, P.; Kroon, J. Conformation of the Xyl-β-(1→2)-Man glycosidic linkage. Structure of 2,4,6-tri-*O*-acetyl-1-*O*-methyl-2-*O*-(2,3,4-tri-*O*-acetyl-β-D-xylopyranosyl)-β-D-mannopyranose. Acta Crystallogr., Sect. C **1990**, *46*, 2171-2174.

35. Taga, T.; Inagaki, E.; Fujimori, Y.; Fujita, K. The crystal and molecular structure of β-D-fructofuranosyl α-D-xylopyranoside. Carbohydr. Res. **1992**, *241*, 63-69.

36. Il'in, S.G.; Lindeman, S.V.; Struchkov, Y.T.; Levina, E.V.; Stonik, V.A.; Elyakov, G.B. Crystalline and molecular structure of 24-*O*-(2,4-di-*O*-methyl-β-D-xylopyranoseyl-(1-2)-α-L-arabinofuranosyl)-5α-cholestan-3β-4β-6α,8,15β,24S-hexaol hydrate. Dokl. Akad. Nauk **1992**, *323*(2), 290-293.

37. Le Questel, J.Y.; Mouhous-Riou, N.; Pérez, S. The crystal and molecular structure of 4-cyanophenyl and 4-nitrophenyl β-D-xylopyranosides. Carbohydr. Res. **1994**, *265*, 291-298.

38. Tomić, S.; van Eijck, B.P.; Kojić-Prodić, B.; Kroon, J.; Magnus, V.; Nigović, B.; Laćan, G.; Ilić, N.; Duddeck, H.; Hiegemann, M. Synthesis and conformational analysis of the plant hormone (auxin) related 2-(indol-3-yl)ethyl and 2-phenylethyl β-D-xylopyranosides and their 2,3,4-tri-*O*-acetyl derivatives. Carbohydr. Res. **1995**, *270*, 11-32.

39. Kanie, O.; Takeda, T.; Hatano, K. Molecular and crystal structure of methyl 2,3,4-tri-*O*-acetyl-β-D-xylopyranosyl-(1→2)-3-*O*-benzyl-4,6-*O*-benzylidene-α-D-mannopyranoside. Carbohydr. Res. **1995**, *276*, 409-416.

40. Takeda, T.; Gonda, R.; Hatano, K. Constitution of lucumin and its related glycosides from *Calocarpum sapota* Merrill. Chem. Pharm. Bull. **1997**, *45*(4), 697-699.

41. Venugopalan, N.; Noguchi, K.; Okuyama, K.; Kitamura, A.; Takeo, K. Molecular and crystal structure of ethyl 2,3,4-tri-*O*-acetyl-β-D-xylopyranosyl-(1→3)-2,4-di-*O*-acetyl-1-thio-β-D-xylopyranoside. Carbohydr. Res. **1998**, *306*, 563-565.

42. James, V.J.; Stevens, J.D.; 1,2,3,4-Tetra-O-acetyl-β-D-arabinopyranose. $C_{13}H_{18}O_9$. Cryst. Struct. Commun. **1974**, *3*, 19-22.

43. James, V.J.; Stevens, J.D.; 1,2,3,4-Tetra-*O*-acetyl-α-D-arabinopyranose $C_{13}H_{18}O_9$. Cryst. Struct. Commun. **1974**, *3*, 187-190.

44. McConnell, J.F.; Schwartz, A.; Stevens, J.D. Methyl β-D-arabinopyranoside, $C_6H_{12}O_5$. Cryst. Struct. Commun. **1979**, *8*, 19-25.

45. Terzis, A. α-L-Arabinose-calcium chloride tetrahydrate, $C_5H_{10}CaCl_2O_5 \bullet 4H_2O$. Cryst. Struct. Commun. **1978**, *7*, 95-99.

46. Takagi, S.; Jeffrey, G.A. The crytal structures of methyl α-L-arabinopyranoside and methyl β-L-arabinopyranoside. Acta Crystallogr., Sect. B **1978**, *34*, 1591-1596.

47. Longchambon, F.; Gillier-Pandraud, H.; Wiest, R.; Rees, B.; Mitschler, A.; Feld, R.; Lehmann, M.; Becker, P. Etude structurale et densité de déformation electronique X-N à 75 K dans la région anomère du β-DL-arabinose. Acta Crystallogr., Sect. B **1985**, *41*, 47-56.

48. Sakata, K.; Yamauchi, H.; Yagi, A.; Ina, K.; Párkányi, L.; Clardy, J. 2-*O*-(β-L-Arabinopyranosyl)-*myo*-inositol as a main constituent of tea (*Camellia sinensis*). Agric. Biol. Chem. **1989**, *53*, 2975-2979.

49. Tomić, S.; van Eijck, B.P.; Kroon, J.; Kojić-Prodić, B.; Laćan, G.; Magnus, V.; Duddeck, H.; Hiegemann, M. synthesis and conformational analysis of 2-(indol-3-yl)ethyl α-L-arabinopyranoside and its 2,3,4-tri-*O*-acetyl derivative. Carbohydr. Res. **1994**, *259*, 175-190.

50. Popek, T.; Mazurek, J.; Lis, T. 1-*O*-Benzyl-β-L-arabinopyranose, 1-*O*-benzyl-3,4-*O*-isopropylidene-β-L-arabinopyranose and 1-*O*-benzyl-2-*O*-benzoyl-3,4-*O*-isopropylidene-β-L-arabinopyranose. Acta Crystallogr., Sect. C **1996**, *52*, 1558-1563.

51. Martínez-Váquez, M.; García-Argáez, A.N.; Bueno, J.L.; Espinosa, G.; Calderon, J.S. Two isomeric glycoside sesquiterpenes from *Machaeranthera tanacetifolia*. Phytochemistry **1998**, *48*(7), 1221-1224.

52. Herpin, P.; Famery, R.; Augé, J.; David, S. Etude structurale du tétra-*O*-acetyl-α-D-lyxopyranose, $C_{13}O_9H_{18}$. Acta Crystallogr., Sect. B **1976**, *32*, 215-220.

53. Evdokimov, A.G.; Frolow, F. Methyl α-D-lyxopyranoside. Acta Crystallogr. Sect. C **1996**, *52*, 3218-3219.

54. Nordensen, S.; Takagi, S.; Jeffrey, G.A. β-L-Lyxopyranose: A neutron diffraction refinement. Acta Crystallogr. Sect. B **1978**, *34*, 3809-3811.

55. James, V.J.; Stevens, J.D.; Methyl 2,3,4-tri-*O*-acetyl-β-D-lyxopyranoside $C_{12}H_{18}O_8$. Cryst. Struct. Commun. **1981**, *10*, 719-722.

56. French, A.D.; Kelterer, A.-M.; Cramer, C.J.; Johnson, G.P.; Dowd, M.K. A QM/MM analysis of the conformations of crystalline sucrose moieties. Carbohydr. Res. **2000**, *326*, 305-322.

Table 1. MM3 energies, puckering parameters, and proton-proton coupling constants for the MM3 local minima of xylopyranose, lyxopyranose and arabinopyranose.

Conformer	Puckering Parameters			MM3 Energies, kcal/mol		x_i^a	Coupling Constants, Hz				
	q, Å	θ, deg	ϕ, deg	Steric	Relative		J_{12}	J_{23}	J_{34}	J_{45d}	J_{45u}
α-xylopyranose											
$^4C_1$	0.561	3.42	236.87	8.935	0.000	0.949	3.5	9.0	8.6	10.6	5.9
$^1C_4$	0.558	172.01	202.47	10.668	1.733	0.050	1.2	3.4	2.9	2.2	1.1
$^5S_1$-^{25}B	0.723	88.06	102.07	13.807	4.872	0.000	2.5	7.0	0.3	2.8	0.7
$^1S_3$	0.780	92.30	206.08	13.945	5.009	0.000	3.3	5.4	9.1	7.2	9.4
^2S_O	0.762	89.52	152.04	14.003	5.068	0.000	5.2	9.9	5.3	1.2	4.2
$^1S_5$	0.743	86.45	264.18	15.865	6.930	0.000	1.2	0.2	6.3	10.6	4.4
$^OS_2$	0.729	90.14	329.47	16.224	7.289	0.000	3.5	4.8	0.8	8.1	9.1
Conformational ave.				9.025			3.4	8.8	8.3	10.1	5.7
Exp.[b]							3.7	9.8	9.1	10.2	5.1
β-xylopyranose											
$^4C_1$	0.591	3.01	13.52	7.939	0.000	0.987	7.2	9.0	8.5	10.6	6.0
^2S_O	0.765	88.86	152.14	10.557	2.618	0.012	4.5	9.9	5.6	1.2	4.4
$^1C_4$	0.519	178.07	175.91	11.748	3.809	0.002	2.5	3.1	3.1	2.2	1.2
$^5S_1$	0.713	85.19	272.57	16.390	8.451	0.000	2.9	0.4	5.2	10.6	4.7
$^3S_1$	0.738	84.67	32.46	16.768	8.829	0.000	5.5	0.3	3.8	1.3	5.1
$^OS_2$-^{3O}B	0.737	87.38	353.47	17.148	9.210	0.000	1.3	3.7	2.5	5.2	9.3
Conformational ave.				7.975			7.1	9.0	8.5	10.5	6.0
Exp.[b]							7.8	9.2	9.0	10.5	5.6
α-lyxopyranose											
$^4C_1$	0.550	6.83	254.12	9.429	0.000	0.825	2.3	3.1	8.8	5.8	10.6
$^1C_4$	0.568	173.09	220.88	10.353	0.924	0.172	7.3	3.1	3.2	1.1	2.2
^2S_O	0.756	90.76	160.11	12.893	3.464	0.002	0.8	2.1	6.3	5.3	1.4
$^OS_2$	0.750	88.80	323.65	13.670	4.240	0.001	5.0	2.3	0.4	8.5	9.2
Conformational ave.				9.599			3.2	3.1	7.8	5.0	9.1
Exp.[b]							4.9	3.6	7.8	3.8	7.2

Table 1. cont.

Conformer	Puckering Parameters			MM3 Energies, kcal/mol		x_i^a	Coupling Constants, Hz				
	q, Å	θ, deg	ϕ, deg	Steric	Relative		J_{12}	J_{23}	J_{34}	J_{45d}	J_{45u}
β-lyxopyranose											
$^4C_1$	0.579	3.85	358.51	9.499	0.000	0.983	1.3	3.0	8.5	6.1	10.5
$^1C_4$	0.535	174.55	269.88	12.086	2.587	0.012	3.0	2.8	3.0	1.6	2.0
^2S_O	0.742	88.80	151.67	12.640	3.140	0.005	3.6	1.9	5.6	4.5	1.2
$^1S_5$	0.749	90.64	281.48	16.015	6.515	0.000	2.4	4.4	3.0	5.4	10.6
$^3S_1$	0.752	86.94	25.29	16.970	7.471	0.000	3.5	6.0	4.3	5.6	1.4
Conformational ave.				9.546			1.3	3.0	8.4	6.1	10.4
Exp.[b]							1.1	2.7	8.5	5.1	9.1
α-arabinopyranose											
$^1C_4$	0.577	175.43	230.75	8.601	0.000	0.996	7.2	9.1	3.1	1.0	2.3
$^4C_1$	0.538	5.61	253.96	12.013	3.411	0.003	2.2	3.5	2.7	6.0	10.6
$^OS_2$	0.758	91.76	337.28	12.715	4.113	0.001	3.9	10.0	4.6	9.5	6.9
$^1S_5$	0.764	87.99	276.57	15.994	7.392	0.000	7.3	5.6	5.8	4.2	10.6
$^1S_3$	0.762	92.99	209.70	16.001	7.400	0.000	5.1	0.6	2.3	9.3	7.7
Conformational ave.				8.616			7.2	9.0	3.1	1.0	2.4
Exp.[b]							7.8	9.8	3.6	1.3	1.8
β-arabinopyranose											
$^1C_4$	0.544	178.07	0.42	9.402	0.000	0.920	3.5	9.1	3.0	1.1	2.4
$^4C_1$	0.572	5.15	345.30	10.856	1.454	0.078	1.4	3.4	3.0	5.9	10.6
$^3S_1$	0.769	87.82	25.26	13.264	3.863	0.001	3.4	5.7	2.2	5.4	1.4
^2S_O	0.731	88.89	152.17	15.440	6.038	0.000	3.6	4.9	5.4	4.9	1.3
$^1S_5$	0.746	88.36	274.27	15.810	6.409	0.000	2.7	5.5	5.8	4.5	10.6
Conformational ave.				9.521			3.3	8.7	3.0	1.5	3.0
Exp.[b]							3.6	9.3	3.4	1.7	2.5

[a]fraction of conformer in population.
[b]in D_2O.[2]

Figure 1. Location of the characteristic chair, boat, skew, half-chair, and envelope forms of the aldopyranosyl monosaccharides on the Pickett-Strauss energy surface (ϕ,θ).

Figure 2. Ring puckering energy surfaces for D-xylopyranose: (**a**) α-xylopyranose and (**b**) β-xylopyranose. Local minima are labeled with crosses (✕). Ring shapes of crystal structures are labeled with circles (●).

Figure 3. Ring puckering energy surfaces for D-arabinopyranose: (**a**) α-arabinopyranose and (**b**) β-arabinopyranose. Local minima are labeled with crosses (✕). Ring shapes of crystal structures are labeled with circles (●).

Figure 4. Ring puckering energy surfaces for D-lyxopyranose: (**a**) α-lyxopyranose and (**b**) β-lyxopyranose. Local minima are labeled with crosses (✕). Ring shapes of crystal structures are labeled with circles (●).

Figure 5. Selected low-energy chair and skew conformers for D-xylopyranose, D-arabinopyranose, and D-lyxopyranose. Intramolecular hydrogen bonds are shown as dashed lines (H … O distance > 2.0 A).

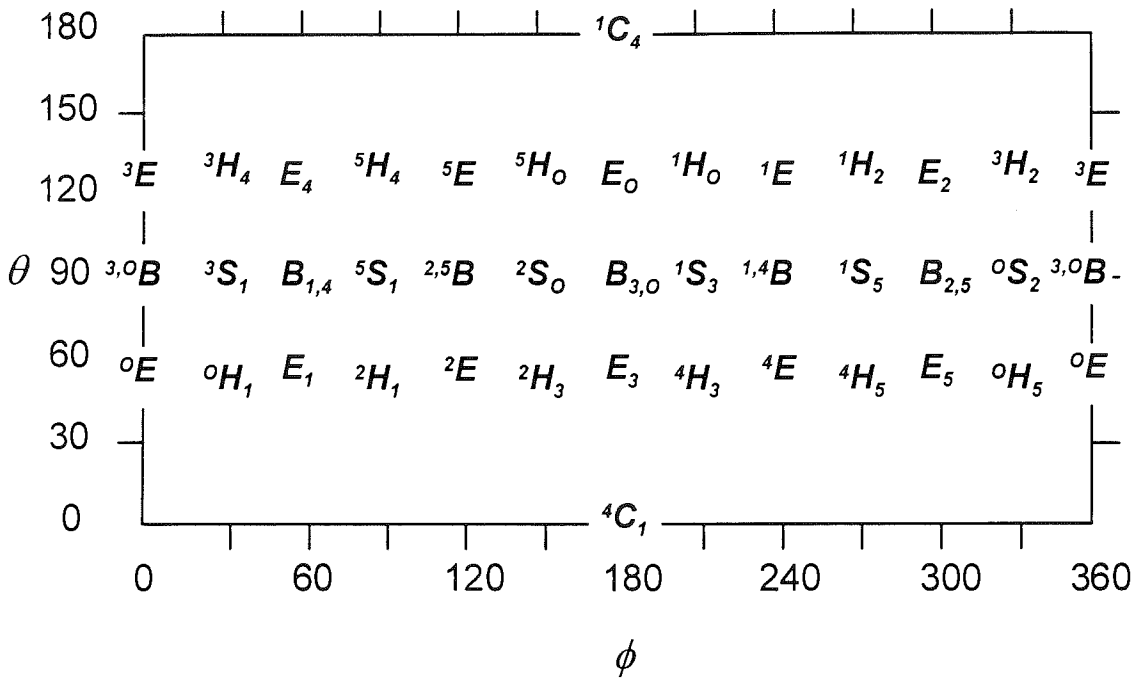

Fig. 1, Dowd et al.

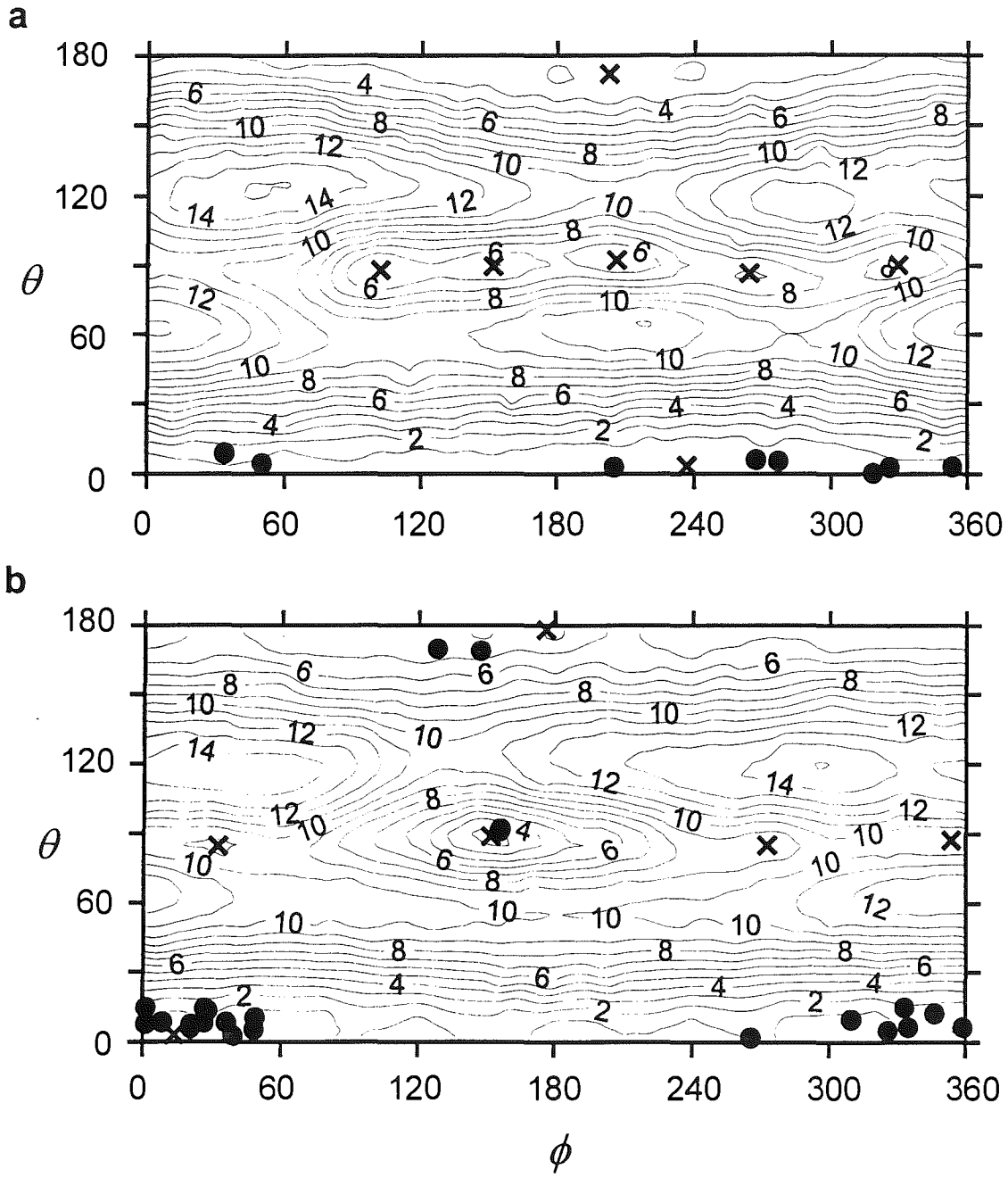

Fig. 2, Doud et al.

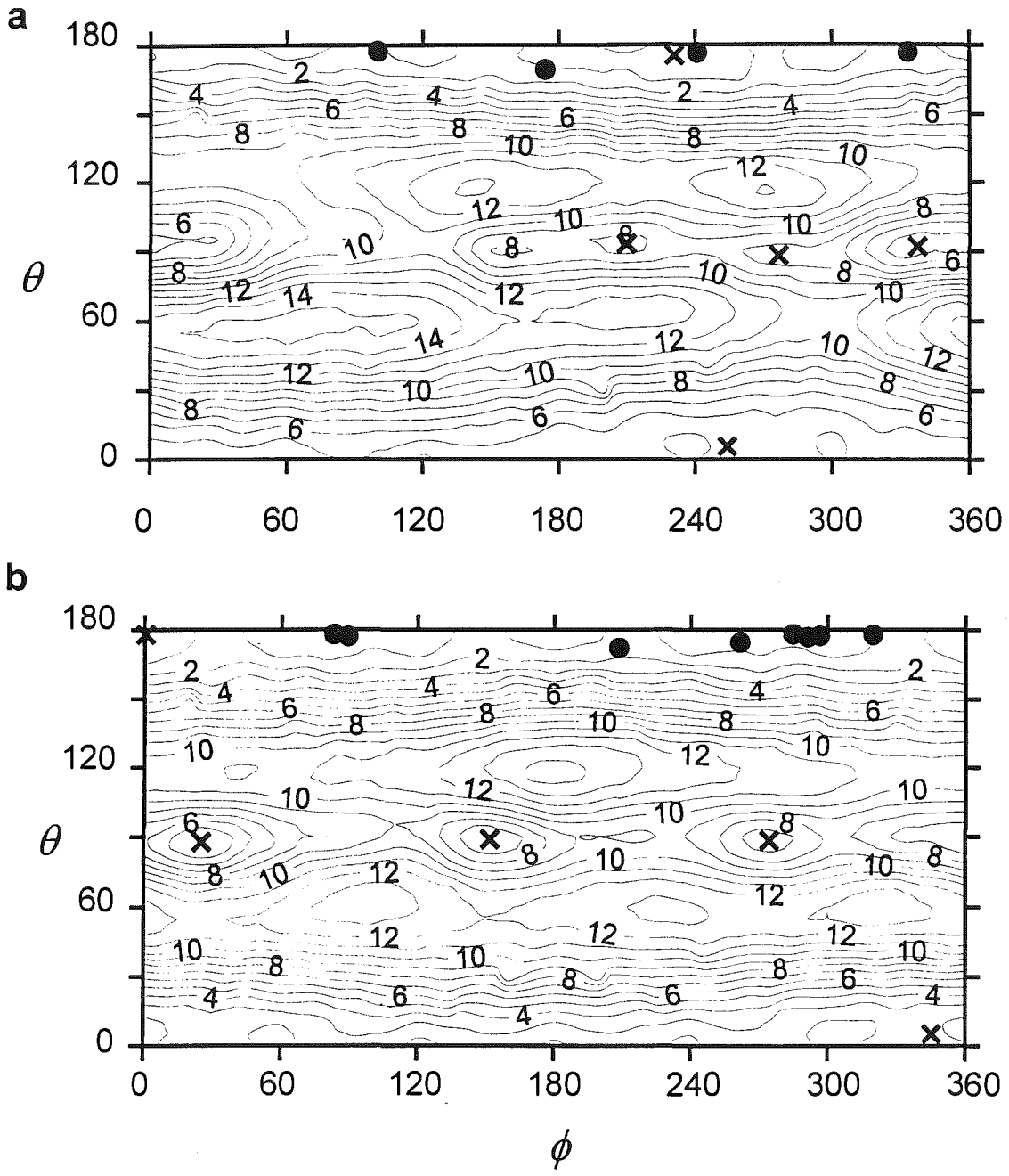

Fig. 3, Dao et al.

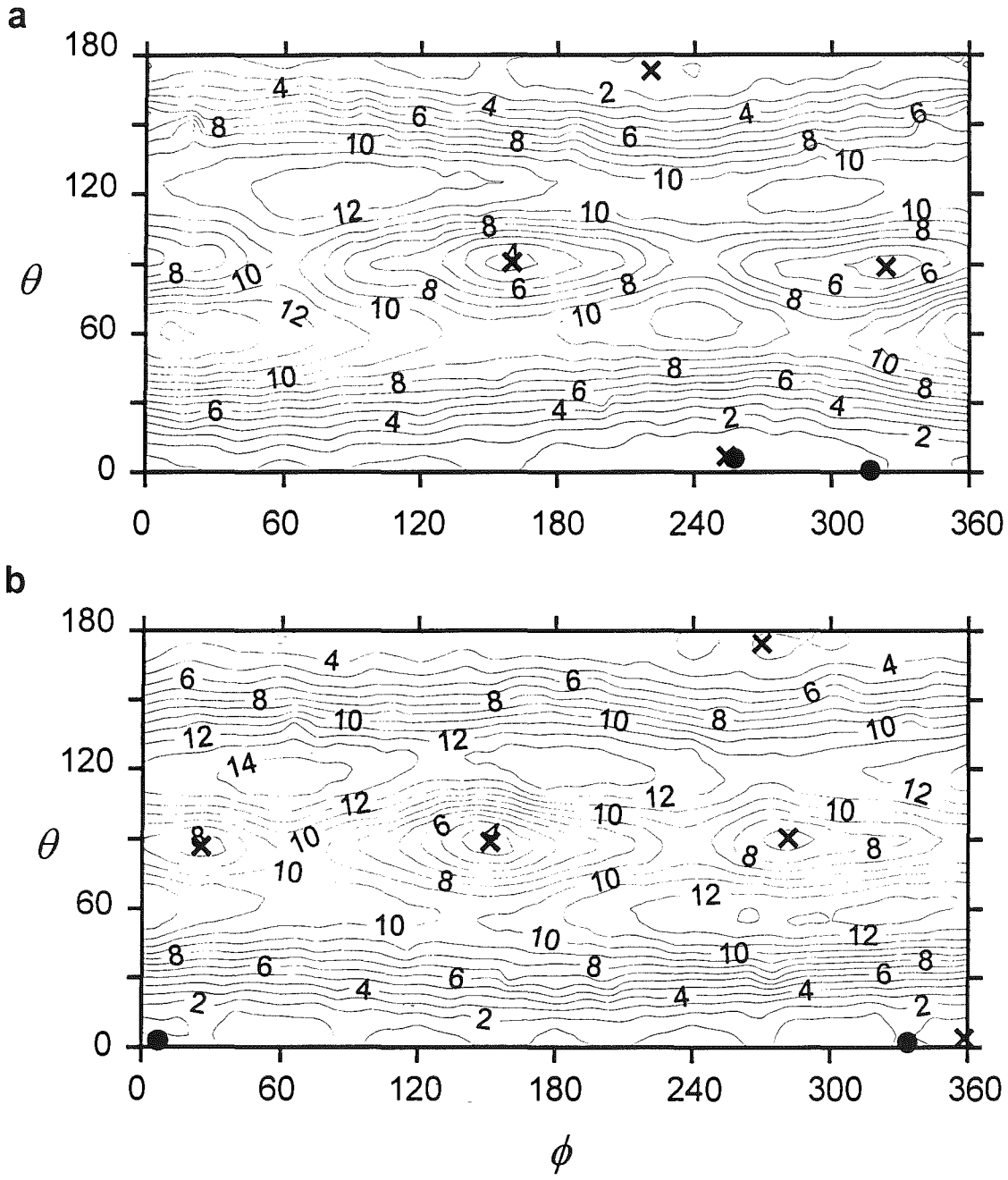

Fig. 4 Dowd et al.

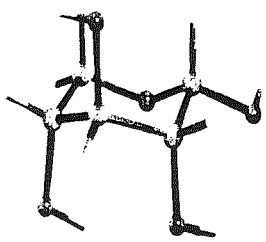

α-xylopyranose
$^1C_4$

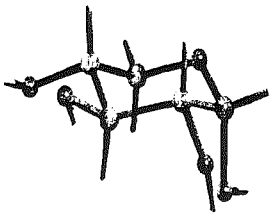

α-xylopyranose
$^4C_1$

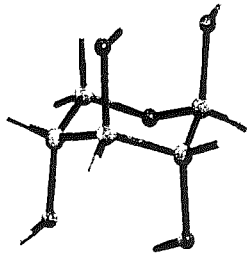

β-xylopyranose
$^1C_4$

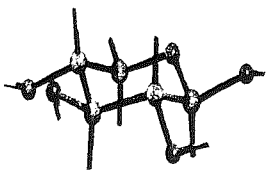

β-xylopyranose
$^4C_1$

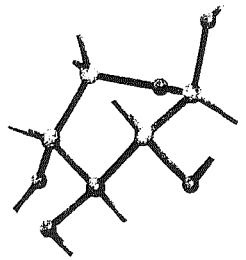

β-xylopyranose
^2S_O

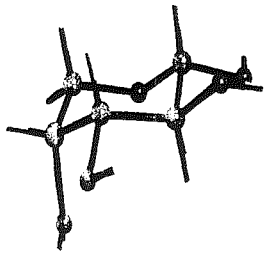

α-arabinopyranose
$^1C_4$

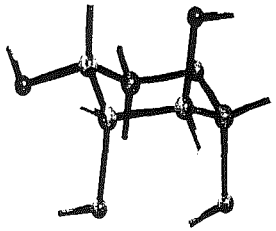

α-arabinopyranose
$^4C_1$

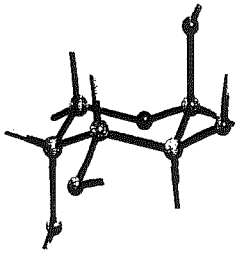

β-arabinopyranose
$^1C_4$

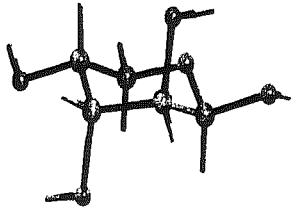

β-arabinopyranose
$^4C_1$

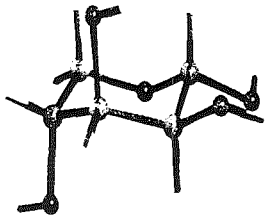

α-lyxopyranose
$^1C_4$

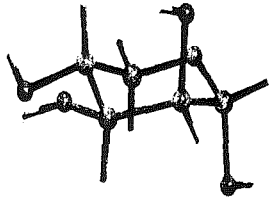

α-lyxopyranose
$^4C_1$

β-lyxopyranose
$^1C_4$

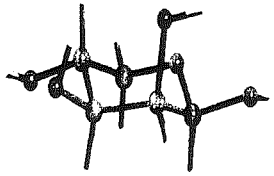

β-lyxopyranose
$^4C_1$